1997 ASME Fluids Engineering Division Summer Meeting
FEDSM'97
June 22 - 26, 1997

FEDSM97-3012

COMPUTER SIMULATIONS OF ULTRASONIC FLOW METER PERFORMANCE IN IDEAL AND NON-IDEAL PIPEFLOWS

T. T. Yeh and G. E. Mattingly
Fluid Flow Group
Process Measurements Division
Chemical Science and Technology Laboratory
National Institute of Standards and Technology
Gaithersburg, Maryland 20899, USA
Phone: 301-975-5953, Fax: 301-258-9201, e-mail: ttyeh@nist.gov

ABSTRACT

This paper describes flow measurement performance prospects for the dual-sensor, travel-time ultrasonic technique, which is the principle of operation of high accuracy ultrasonic flowmeters. Computer models of dual sensor ultrasonic flowmeters are developed using both straight line wave propagation and wave ray paths in pipe flow. The effects of curved acoustic paths and various meter configurations on performance are assessed. Results indicate that the assumption of straight line wave propagation paths is quite adequate for small Mach numbers, i.e. smaller than 0.1. The flow profile sensitivities of the meters are investigated for several analytical velocity profiles in high Reynolds number (Re ~10^6) pipe flows. Meter prospects are also assessed in a turbulent, high Reynolds number pipeflow from a single elbow that is computed using a commercially available computer code. Results from these meter simulations indicate that installation locations and orientations of dual sensor ultrasonic flowmeters are critical in attaining satisfactory levels of meter performance. Results also suggest that multi-path flowmeters are probably more desirable for assuring high levels of metering accuracy and profile insensitivity.

NOMENCLATURE

C	Speed of sound
C_I	Meter constant = W_b/V_I
D	Pipe diameter
F_n	Piping configuration parameter
M_f	Flow Mach number =W_b/C
Re	Reynolds number
V	Vectorial fluid velocity, = (u,v,w)
V_s	Fluid velocity averaged along the path
V_I	Meter indication velocity
V_o	Taylor vortex strength
V_θ	Angular velocity of a vortex
W_b	Average or bulk velocity
b	Radial offset of chordal path
e	Unit vector tangent to **s**, =(e_x,e_y,e_z)
e_x, e_y, e_z	Direction cosines of ultrasonic path
$\mathbf{e}_s$	Unit vector between emitter and receiver
r	Radial coordinate
r_o	Taylor vortex core size
s	Vectorial position of ultrasonic path
s	Scale length of ultrasonic path
t_{ij}	Time of flight from i to j
u,v,w	Velocity components in x,y,z respectively
x,y,z	Cartesian coordinates
z_m	Meter axial location
α	Meter azimuthal angle
ϕ	Meter axial angle

INTRODUCTION

Ultrasonic technology has great potential for improving flow metering. The objective of this study is to understand and assess ultrasonic technology to realize some of this potential. The approach used is based on computer modeling methods to analyze and understand this technology in these conditions. This paper focuses on flow measurement performance prospects for dual-sensor, travel-time ultrasonic techniques applied to high Reynolds number pipe flows of incompressible fluid that are typical of practical metering conditions. The paper is intended to provide a comprehensive understanding of the operational principle of ultrasonic flowmeters and to serve as a foundation to advance the development of ultrasonic flowmeters. A well-designed ultrasonic flowmeter requires

understanding many practical topics such as the physics of sound propagation, reflection, and absorption phenomena, as well as signal processing and array considerations, ambient noise and reverberation effects, and scattering problems. In this investigation, we focus on numerical techniques to simulate meter performance due to various pipeflow profiles. The technical approach is 1) to develop numerical simulations of travel-time ultrasonic flowmeters (NUSFM), 2) to model the selected turbulent pipeflows via computational fluid dynamics(CFD), and 3) to use NUSFM simulations in the modeled pipeflows to investigate and understand the performance of this type of ultrasonic flowmeter.

NUMERICAL ULTRASONIC FLOWMETER MODELING

There are several types of ultrasonic flowmeters; these use both travel-time and Doppler techniques. In this paper, we consider the dual-sensor, travel-time technique. This technique can be arranged via sensors clamped on the outside of pipe or it can be used with sensors mounted through the pipe wall to operate in contact with the flow stream, i.e. wetted. Here, we consider only flow field effects, i.e. the wetted sensor type flowmeter. Figure 1 sketches the ultrasonic flowmeter. The upstream and downstream sensor locations and signal paths are shown. The objective of the study is to develop a NUSFM so that various velocity profile effects can be investigated.

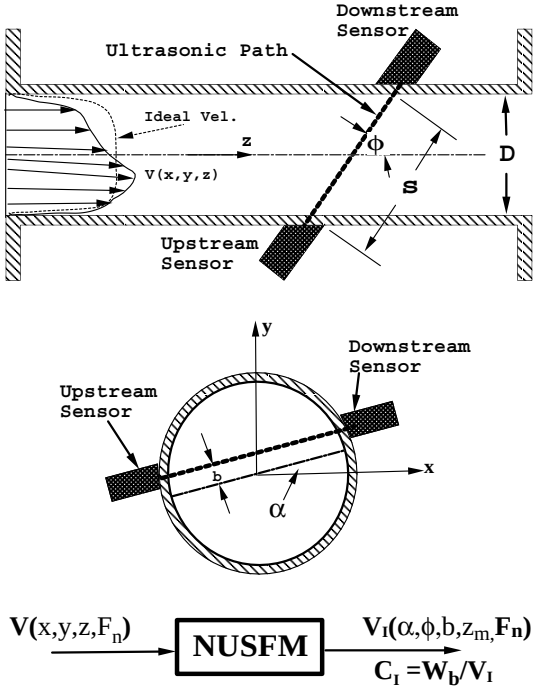

Figure 1. Schematic diagram of a Dual-Sensor Ultrasonic Flowmeter

Ultrasonic Flowmeter Models

Travel-time ultrasonic flowmeters measure the time difference between upstream and downstream pulse propagation times. The basic equations for the ultrasonic flowmeter can be written as:

$$\int_1^2 dt = t_{12} = \int_1^2 \frac{ds}{C+\mathbf{V}\cdot\mathbf{e}} \approx \frac{s}{C+V_s}$$
$$t_{21} = \int_1^2 \frac{ds}{C-\mathbf{V}\cdot\mathbf{e}} \approx \frac{s}{C-V_s} \quad (1)$$

Thus, from the above equations, we have

$$V_I = \frac{V_s}{\cos(\phi)} = \frac{s}{2\cos(\phi)}\left(\frac{1}{t_{12}} - \frac{1}{t_{21}}\right)$$
$$C = \frac{s}{2}\left(\frac{1}{t_{12}} + \frac{1}{t_{21}}\right) \quad (2)$$

These results show that the ultrasonic flowmeter technique not only determines the fluid velocity, it also determines the speed of sound. Thus, the technique can be used to measure other fluid properties (such as temperature, etc.) if the relationship of the desired property to the speed of sound is known. The configuration parameters for dual-sensor ultrasonic flowmeters included in the model are the offset b; the azimuthal angle α and the axial angle ϕ. Since the fluid velocity **V** depends on the pipe configuration F_n and axial location z_m, the meter indication V_I and the meter constant C_I will be functions of α, ϕ, b, z_m and F_n.

Signal Path Model

As shown in Fig.1, a straight line path connecting the two sensors is normally assumed for modeling both upstream and downstream signals. However, in general, the ultrasonic signal paths will deviate from straight lines and the signal paths for upstream and downstream directions will be different. To study the effects of these curved rays on the performance of ultrasonic flowmeters, computer models of dual sensor ultrasonic flowmeters are developed using both straight line propagation and wave ray theory in pipe flow. These two models are:

1) Straight line path

$$\mathbf{s} = s\mathbf{e}_s, \quad and \quad \frac{ds}{dt} = (C + \mathbf{V}\cdot\mathbf{e}_s) \quad (3)$$

where $\mathbf{e}_s$= constant, is a unit vector between the two sensors.

2) Ray theory path (Boone,1963)

$$\frac{d\mathbf{s}}{dt} = C\mathbf{e} + \mathbf{V}$$
$$\frac{d}{dt}\left(\frac{\mathbf{e}}{C+\mathbf{V}\cdot\mathbf{e}}\right) = -\frac{\nabla C + e_x\nabla u + e_y\nabla v + e_z\nabla w}{C+\mathbf{V}\cdot\mathbf{e}} \quad (4)$$

Here ∇ denotes vector gradient. The ray theory approximation assumes that the vector gradients are slowly varying functions of space. Eqn.4 shows that both the sound speed gradient and the velocity gradient (tensor) affect the propagation direction of the ray **e**. However, a uniform velocity and a constant sound speed will result in a straight ray. Ray direction changes in time increase as the speed of sound C decreases. In incompressible flow where the Mach number M_f=0, the ray path is straight. The effects of the Mach number

on the flowmeter performance for constant speed of sound are investigated and reported below.

SELECTED PIPEFLOW PROFILES

The numerical simulation of ultrasonic flowmeter performance requires a complete 3-D pipe flow field and its gradients. Performance prospects for dual-sensor, travel-time ultrasonic techniques are investigated for high Reynolds number pipe flows of incompressible fluid. In what follows, both analytical velocity profiles and a common industrial pipeflow are used.

Analytical Pipeflow profiles

Various analytical pipeflow velocity profiles can be selected to test the sensitivity to such effects and investigate the resulting performance of dual-sensor meters. In general, the complete velocity field can be divided into axial and cross flow components. Cross or swirl flows are simulated by the classic Taylor vortex model (Dryden,et al, 1956),

$$V_\theta = V_o r_v \exp(-r_v^2) \tag{5}$$

where $r_v=r_c/r_o$ and r_c is the distance from the vortex center. This distribution does not directly exhibit the velocity variation that is inverse with the radius r_c. Instead, it gives more emphasis to the solid body rotation near the axis of rotation and the exponential decay further from this center. In our pipe flow, it appears that these features more closely model the characteristics of our vortices(Mattingly & Yeh, 1988,1992)

Symbols used to identify the profiles are:

(1) Unif: Uniform axial velocity $w/W_b=1.0$,

(2) Laminar: Parabolic profile, $w/W_b=2\,(1-(2r/D)^2)$,

(3) PowerLaw: $w/W_b = C_n\, r^{1/n}$, where C_n is function of the power law exponent n,

(4) BM: Fully developed profile given by Bogue and Metzner(1963), with modified linear wall profile,

(5) RC: Profile given by Reichardt (1951),

(6) LOG: $w^+ = 5.75 \log(y^+) + 5.55$, with linear wall profile,

(7) GIL: Profile given by Gilmont (1996),

(8) Skx:: skew w, $w/W_b=1.0+x$,

(9) 1ed: a single Taylor eddy at r=0 with $V_o/W_b=0.7$, $r_0/D=0.2$, and $w/W_b=1.0$,

(10) 2ed: two Taylor eddies on y=0 with $V_o/W_b=0.5$ and $r_0/D=0.15$, and $w/W_b=1.0$,

(11) 2ed-sky: same as 2ed above, except $w/W_b=1.0-y$.

The wall profile is given by $w^+=y^+w^{+20}$ for $y^+ < 20$, where w^+ and y^+ are, respectively, the axial velocity and wall distance based on wall units, and w^{+20} is the velocity at $y^+=20$.

Non-Ideal Pipeflow

To investigate meter performance in a more practical, non-ideal, turbulent pipeflow, a CFD model of the flow through a single elbow was produced using a commercially available computer code. This uses multi-cuboid blocks with a body-fitted grid. The model conditions are: 3-D, steady state, high Reynolds number, RNG κ-ε turbulence model, a fully developed inlet velocity profile with Laufer's(Laufer, 1952) turbulent kinetic energy and dissipation, a Neumann outlet boundary condition with zero normal gradient, and a synthetic, logarithmic wall profile with a no slip condition. The coordinate system used is right-handed with origin on the pipe centerline in the exit plane of the elbow, y is in the plane of symmetry of the elbow and is directed toward the source of flow to the elbow. Thus, the meter angle $\alpha=0$ aligns with the x axis. The CFD results indicate that these high Reynolds number($Re=3 \times 10^6$) flows differ significantly from the fully developed condition 55 diameters or more downstream of the elbow. Owing to the lack of data, the CFD results for this flow are not validated directly with experimental data. However, the CFD results for a lower Reynolds number($Re= 10^5$) flow have been validated using laser Doppler velocimetry from NIST's ongoing research program on flow meter installation effects(Mattingly & Yeh, 1988,1992).

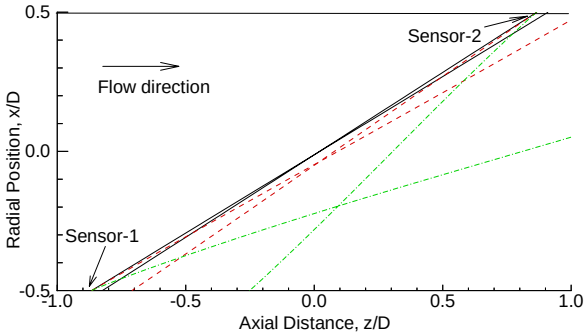

Figure 2. Effects of fluid velocity on ultrasonic rays for the Bogue & Metzner profile for $Re=3 \times 10^6$, b=0, $\phi=30^o$, $\alpha=0$ and y=0 plane. M_f : 0.005 (solid) , 0.02 (dash), and 0.10 (dotdash)

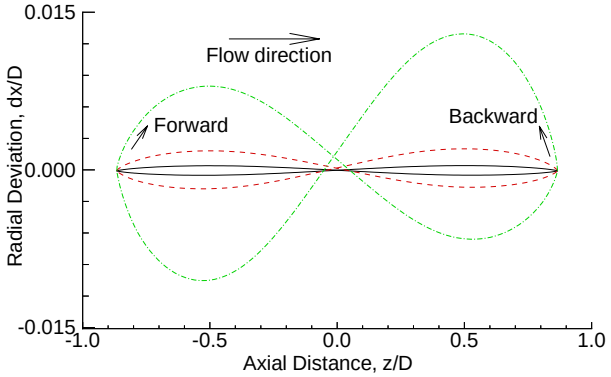

Figure 3. Deviations of ray path from a straight line. (same condition as figure 2).

RESULTS

The effects of curved ray paths on meter performance are investigated first. As indicated above, the meter performance, in general, will depend on α, ϕ, b, and z_m. In this paper, unless

otherwise specified, the nominal values for these parameters are: α=0, ϕ=30°, and b=0. Figure 2 shows narrow band ray paths which are aimed between the two sensors. It shows that the fluid velocity affects the rays and that signals aimed at the other sensor will not hit it. To make contact, different initial angles for the signals are needed. These effects diminish as the Mach number of the flow becomes very small. This indicates that, in principle, narrow beam angles cannot be used with small sensors. When ultrasonic transducers emit a conical wave, the signal starting from an angle different from the straight line direction will reach the receiver. These starting angles are functions of the fluid velocity profiles as indicated by the ray theory, see Eqn.4. Here a multivariable iteration technique is used to find the correct starting angles. Figure 3 shows the effects of fluid velocity on rays by showing the path deviations from a straight line. These deviations show that the ray path depends the flow Mach number. Additional data show the deviations also depend on the axial angle, ϕ. This is true even for fully developed profiles which are independent of axial position z.

It is clear that flow profile affects the ray paths. However, the effects these have on the performance of ultrasonic flowmeters remain to be seen. To answer this question, the flowmeter simulation was run for all the selected analytical velocity profiles as functions of M_f. Figure 4 shows flow profile effects on the meter indication as functions of M_f by showing the meter indication deviations from the straight path case. These results indicate that the assumption of straight line path is quite adequate (deviation < 0.5%) for small Mach numbers(<0.1), except for the case of laminar flow where the M_f is normally very small. Thus, for most practical applications in liquid flow measurements where M_f < 0.005, the straight line assumption seems adequate. Therefore, the results that follow will be for M_f=0.005.

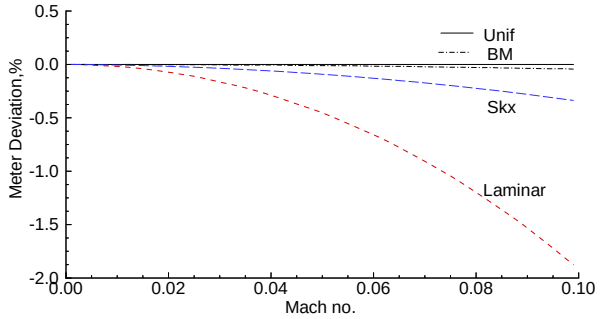

Figure 4. Deviation of the meter indication vs. M_f for α=0, ϕ=30° and b=0. (Values for RC, PowerLaw, LOG, GIL, 1ed, 2ed, and 2ed-sky are between those of BM and Unif and are not shown here for clarity).

Figure 5 shows the profile effects on dual-sensor meter installations. The upper figure shows α angle effects. As expected, the meter indication is constant in axisymmetric flows and is equal to 1.0 for uniform flow. However, it is more interesting to note that the values are equal to 1.0 for both the single swirl(1ed) and pure skew(Skx) flows. There are no angular effects on the indicated velocity for the skew flow, however the double swirl profiles produce large α angle variations in meter indication. The lower figure shows radial offset effects for α=0. The effects of a single swirl are clearly shown and there is no effect in the double swirl flows for different radial offsets. These results indicate that special caution is needed when a chordal path flow meter is used to measure in the presence of cross flows.

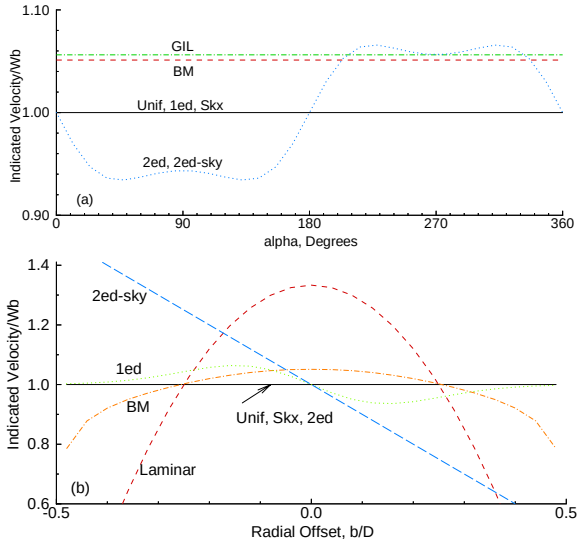

Figure 5. Effects of dual-sensor meter installation on meter indication for α=30°, Re=3 x 10^6, and M_f=0.005. (a) α effects for b=0. (Laminar =1.3334, LOG=1.051, RC=1.0506, PowerLaw =1.048), and (b) b effects for α=0. (Unshown values for LOG, RC, Power Law, and GIL are very close to that of BM)

We have seen that various factors can affect the meter indication. Here we note the two fundamental issues of dual-sensor ultrasonic flowmeters. The first is the error due to the cross flow components. The effective velocity seen by the flowmeter is

$$V_s = \mathbf{V}\cdot\mathbf{e}_s = ue_x + ve_y + we_z$$
$$V_I = V_s / e_z = w + (ue_x + ve_y)/e_z \qquad (6)$$

The desired indication is the axial velocity, w. However, the indicated velocity contains extra terms from the cross components u and v. The cross component increases as ϕ increases or as e_z decreases. To get the correct meter indication, we will have to either 1) make sure the integration result of the cross component is canceled, or 2) determine the cross flow contribution and then subtract it. Figure 6 shows the effective fluid velocity for both the axial and the cross

components as seen by the dual sensor meter for a 2ed-sky profile. The value for the uniform axial value ($e_z=\cos(\phi)$) is also given for reference. In this double swirl flow, when the sensor angle $\alpha=0$, no error appears for either component. When the angle α is non-zero, the error due to the cross component is always negative along the path and therefore the integral is non zero. However, the deviation of the axial component is symmetrical around the center of the path, the end result is canceled and pure skew flow does not affect the meter performance.

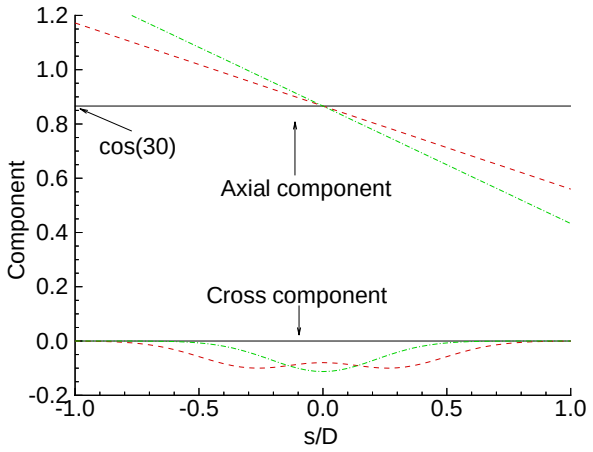

Figure 6. Effective velocity as seen by the meter for a 2ed-sky profile along the path length s. α : 0^o (solid), 45^o (dashed) and 90^o (dashdot). Axial Comp.=we_z, Cross Comp.=ue_x+ve_y

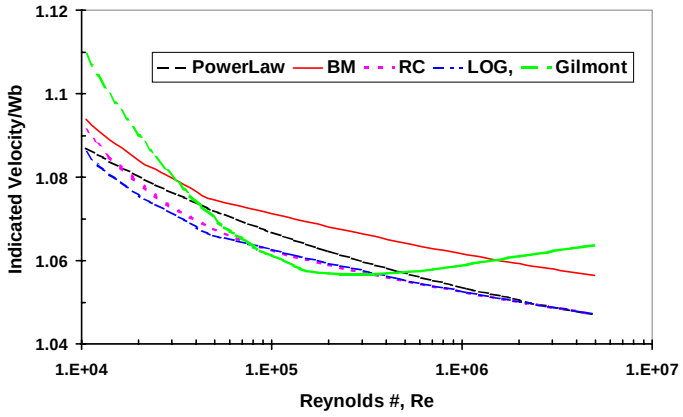

Figure 7. Indicated meter velocity vs. Reynolds no. (Laminar=1.3334, and all others=1.00)

The second issue of the dual-sensor ultrasonic flowmeter is to interpret the area-averaged velocity from the measured line velocity V_I . To do the interpretation, a fully developed pipe flow profile is normally assumed and thus the accuracy of the meter will depend on the assumed profile. Figure 7 shows meter indication vs. Reynolds no.. This shows that meter accuracy depends on the selection of a particular assumed profile for correcting the meter constant.

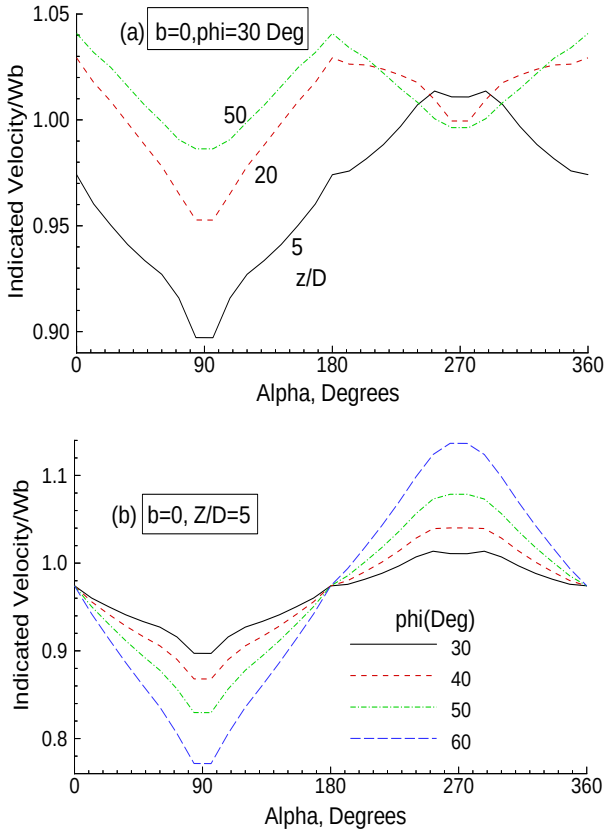

Figure 8. Indicated velocity of the dual-sensor flowmeters downstream of a single elbow vs. α for Re=3 x 10^6, M_f =0.005 and b=0.

CFD results are also used to simulate flowmeter response for the flow from the single elbow in various meter installation parameters. Fig. 8 shows α effects on meter indication, while Fig. 9 shows the radial offset and axial distance effects. These results indicate that the meter indication strongly depends on the meter installation orientation and location. When a meter is located near the single elbow (z/D=5), the meter indication, as shown in Fig.8(a), varies from a minimum of 0.9 near $\alpha=90^o$ to a maximum of 1.01 near $\alpha=270^o$. Both these values are smaller than the reference value of 1.05 for a BM profile, which is often assumed to interpret the meter indication. Since the meter indication is always lower than the average velocity (~ 1.05 for a BM profile), no installation angle can be found to produce a correct velocity. Larger α dependence is found for a larger ϕ as shown in Fig. 8(b). The deviation is as large as 35% for $\phi=60^o$. The large variation of the meter indication with α is mainly due to the cross flow component produced by the double eddies in the single elbow flow(see also Eqn.6). This variation is similar to that of 2ed flow shown in Fig.5(a). The below average meter indication can be seen more clearly from Fig.9(a) at b=0 for the single flow, which has a slow core and fast flow near the wall.

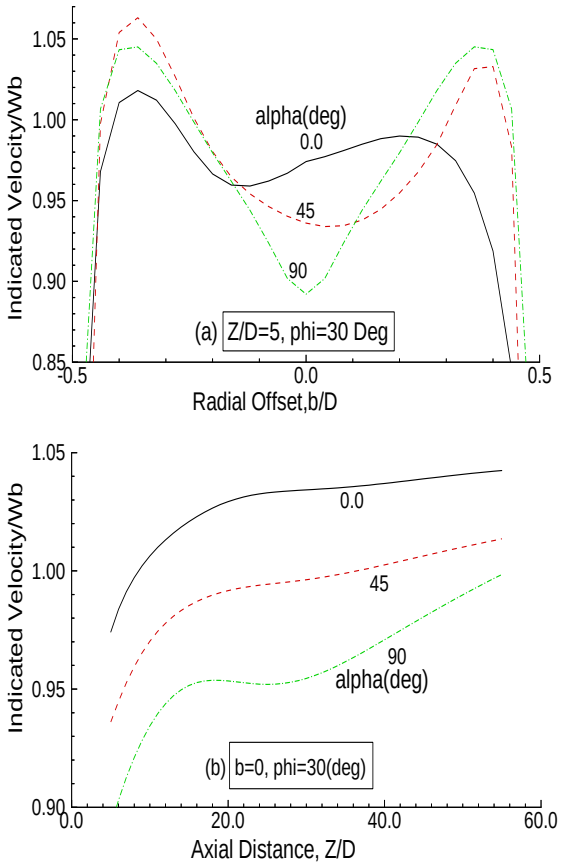

Figure 9. Indicated velocity of the dual-sensor flowmeter downstream of a single elbow for Re=3 x 10^6, M_f =0.005.

Fig.9(b) shows the meter indication is still a strong function of α and thus indicates that the flow is not fully developed even at z/D=55. All these results indicate that installation location and orientation are critical to satisfactory levels of meter performance. These results and others like them for other practical conditions can be used to generate installation guidelines for paper standards for this measurement method. Results also show that multi-path flowmeters are probably more desirable to assure high levels of metering accuracy and profile insensitivity.

SUMMARY

Dual sensor, travel-time ultrasonic flowmeters have been modeled numerically in a range of conditions. Both straight line waves and ray theory paths have been used in the model. The reported meter simulation results quantify the ranges of metering accuracy that can be obtained in ideal pipeflows when different assumptions are made for a range of ideal pipe flow profiles. Simulation results quantify flow meter performance variations relative to that in ideal flows when non-ideal flows are considered.

The results indicate that dual sensor ultrasonic flowmeters have a high degree of flow profile sensitivity in the selected flows. The performance of the flowmeter is a function of the parameters: α, ϕ, b, and z_m in addition to upstream pipe configuration. For most practical applications in liquid flows (M_f < 0.1), the assumption of straight line wave propagation is quite adequate. For the flow from a single elbow, the meter indication strongly depends on the meter installation orientation and location. Near the elbow, the variation could be as large as 35% due to the cross flow effects. In many cases, no azimuthal angle can be found to produce ideal performance because the zero radial offset meter senses the slow center core flow and thus the meter indication is lower than the average flow for all α angles. These results confirm that installation locations and orientations of these meters are critical to metering accuracy and multi-path flowmeters are desirable for high accuracy and profile insensitivity.

ACKNOWLEDGMENTS

The technical contributions of Mr. P. I. Espina and several discussions of data interpretation with Dr. Minye Liu of Cray Research, Inc. are gratefully acknowledged.

REFERENCES

Bogue, D.C. and Metzner, A.B., 1963, "Velocity Profiles in Turbulent Pipe Flow", *I&EC Fundamentals*, Vol. 2, No. 2.

Boone, M.M. and Vermaas, E.A., 1991, "A New Ray-Tracing Algorithm for Arbitrary Inhomogeneous and Moving Media, Including Caustics", *J. Acoustic Soc. Am.*, 90(4), pt. 1.

Dryden, H., Murnaighan, F.D. and Bateman, H., 1956, "Hydrodynamics", *Dover Publ.Co.*, New York, NY, P.213.

Gilmont, R., 1996, "Velocity Profile of Turbulent Flow in Smooth Circular Pipes", *Measurements and Control*, pp. 96-103.

Laufer, J., 1952, "The Structure of Turbulence in Fully Developed Pipe Flow", *NBS Report*. 1974

Mattingly, G.E. and Yeh, T.T., 1988, "NISTs Industry-Government Consortium Research Program on Flowmeter Installation Effects: Summary Report with Emphasis on Research Period July - December, 1987", *NISTIR* 88-3898, Nov., 1988

Mattingly, G.E. and Yeh, T.T., 1992, "Flowmeter Installation Effects Due to Several Elbow Configurations", *Proceedings of the 2nd International Symposium on Fluid Flow Measurement* , pp. 271-283.

Reichardt, V.H., 1951, "Vollstandige Darstellung der turbulenten Ges chwindigkeitsverteilung in glatten Leitungen", *Z.angew. Math. Mech.*, Bd.31, Nr.7